Effects of pressure on the non-linear viscoelastic behaviour of polymers: 2. Poly(vinyl acetate)

S. H. Joseph* and R. A. Duckett
Department of Physics, University of Leeds, Leeds LS2 9JT, UK
(Received 27 October 1977; revised 21 February 1978)

Torsional stress–strain measurements on poly(vinyl acetate) are described covering a range of strain rates and temperatures under superposed hydrostatic pressures up to 450 MN/m^2. The mechanical behaviour is dominated by the α relaxation which can be swept through the experimental time scale by the application of pressure. Analysis of the small strain behaviour reveals an approximate time–temperature–pressure equivalence with quantitative agreement with the findings of previous workers. Large strain experiments at atmospheric pressure show that by increasing strain rate over a wide range the small strain measurements indicate a transition from rubbery to glassy behaviour, and the large strain measurements reveal the appearance of a shear yield stress. The Ree–Eyring equation is used to link, in a quantitative manner, the small and large strain properties although detailed analysis of the data shows that the non-linear viscoelastic response encompasses several discrete mechanical processes.

INTRODUCTION

In part one of this study[1] it was shown that pressures of up to 450 MN/m^2 cause significant changes in the mechanical properties of polypropylene (PP) at both high and low strains, and that these changes are directly associated with the β transition which occurs at around 150 MN/m^2 pressure at room temperature. Interpretation of the data from PP is complicated by the semicrystalline nature of the material and the breadth of the transition.

In this paper, experiments on poly(vinyl acetate) (PVAc) are described. This material, which has a dilatational glass transition temperature (T_g) between 25° and 32°C has been tested in torsion under hydrostatic pressure. Use of elevated temperatures enables measurements above T_g to be made, thus providing the possibility of investigating the transition as brought on by an application of pressure.

The α relaxation of PVAc which is associated with the glass transition has been studied by dielectric and mechanical experiments in great detail and has been reviewed by McCrum *et al.*[2]. Dynamic mechanical measurements[3] indicate a comparatively narrow relaxation spectrum and time–temperature superposition following the WLF equation. O'Reilly[4] has interpreted dielectric relaxation measurements under superposed hydrostatic pressure in terms of a compressibility of free volume which varies with pressure, and suggested an approximate pressure–temperature equivalence of 0.22°C (MN/m^2)$^{-1}$. More extensive data from dynamic bulk modulus measurements[5] at various static pressures and temperatures showed that the behaviour was more complex and that the WLF equation applies only imperfectly to the time–pressure–temperature shifts in bulk response.

Torsion pendulum measurements[6] show that the dominant relaxation is the α process. The very small relaxations observed at −100° and −30°C (at ~1Hz) are associated with a total change in shear modulus from 2000 to 1700 MN/m^2 whereas the α process at approximately 35°C involves a decrease in modulus to below 3 MN/m^2.

Thus PVAc would seem to be an ideal material to study. Its behaviour within 40°C or within pressures of 200 MN/m^2 of the glass transition should be dominated by the α relaxation, and the effects of this relaxation on the non-linear viscoelasticity of the material should most clearly be seen.

EXPERIMENTAL

The high pressure torsion machine described in part 1 was used to test specimens of PVAc. A rod 40 mm in diameter was melt extruded from granules of Mowilith 60 (molecular weight 380 000) and subsequently machined into specimens as shown in *Figure 1*. These were made as large as possible so as to minimize the error in measuring the small torques consequent on the low modulus above T_g. Machining the material was difficult, but possible if high cutting speeds and plenty of coolant were used so that the polymer remained in the glassy state. Following preliminary tests in which crazing and fracture were observed in torsion on specimens with an 'as-machined' finish, the specimens were polished in the gauge section using Perspex polish numbers 1 and 2, followed by Greygate plastic polish. Care was taken to avoid any temperature rise. The finish achieved was sufficient to

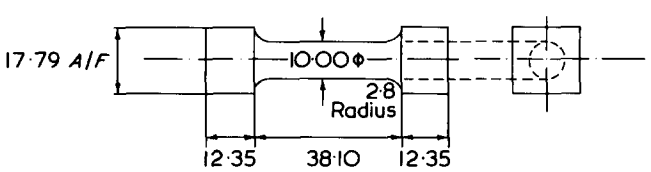

Figure 1 Dimensions of PVAC torsion specimen (mm)

* Present address: Department of Mechanical Engineering, Imperial College of Science and Technology, Exhibition Road, London SW7 2BX, UK.

0032–3861/78/1907–0844$02.00

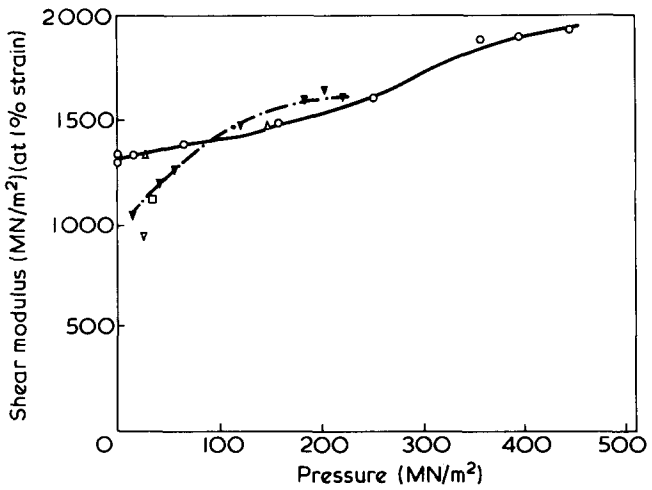

Figure 2 Shear modulus (1%) of PVAc. T = 19.4°C; △, $\ln(\dot{\gamma})$ = −8.3; ○, $\ln(\dot{\gamma})$ = −6.0, T = 30.0°C, ▽, $\ln\dot{\gamma}$ = −8.3; □, $\ln\dot{\gamma}$ = −7.1; ▼, $\ln\dot{\gamma}$ = −6.0

eliminate crazing in air at all the strain rates used. In order to remove absorbed water and to anneal the specimens, they were held under vacuum at 30°C for 10 days, and then stored in a dessicator over calcium chloride at room temperature (22°C).

In tests under pressure it was found that the high pressure fluid, Plexol (diethyl dihexyl sebacate), although not absorbed by PVAc[5], did act as a very severe crazing agent. Despite attempts to exclude the fluid from the specimen surface, crazing could not be entirely eliminated in tests at high strains and elevated pressures. In view of the sensitivity of yield stress measurements to even a limited amount of craze formation[7], discussion of tests under pressure is restricted to the small strain region only: no crazing was seen after such tests.

The dependence of modulus on strain rate, temperature and pressure was investigated, using the pressure-ramp and modulus measurement methods previously described[8]. Strain rates from 0.75×10^{-2} to 1.2×10^{-4} sec^{-1} were used, and pressure-ramps at ramp rates of 1.0×10^{-2}, 0.8×10^{-2} and 0.5×10^{-2} MN/m^2 sec were run at temperatures of 19.4°, 30.0° and 33 9°C, respectively. Temperatures were measured using a specially constructed copper resistance thermometer[8]. In view of the strong dependence of modulus on temperature particular care was taken to ensure that the specimen had reached the bath temperature before test ing. Tests on the modulus at varying times after loading the specimen showed that in the α transition region, a period of 20 min was required before the modulus had stabilized at the level appropriate to the vessel temperature. This effect was minimized by preheating the specimen and grips to the vessel temperature. There is an additional problem of axial creep in the specimen under the weight of the upper grip at elevated temperatures and atmospheric pressure. Using the data below it is estimated that the axial creep at the highest temperature is below 1% in 1 h. Tests were therefore run at 30 to 40 min after the specimen was loaded. No axial strains could be detected in specimens removed after testing.

Torsion tests at up to 30% strain were also performed at 33.9°C and at atmospheric pressure. These were conducted and analysed following the procedure developed for the tests on PP described in part 1[1].

RESULTS

Shear modulus

Time–temperature–pressure equivalence. The shear modulus of PVAc at 19.4°C (*Figure 2*) shows the slight dependence on pressure and strain rate expected of a glassy material. The increase in modulus observed at pressures between 250 and 300 MN/m^2 may correspond to the secondary transition observed at −30°C and atmospheric pressure in torsion pendulum experiments[6]. This gives a shift of 0.18°C $(MN/m^2)^{-1}$, approximately equal to previously observed shift values for the α transition in PVAc[9]. The material is nearing the α transition at 30.0°C and shows some rate dependence at pressures less than 50 MN/m^2 (*Figure 2*). The intersection of the two curves seen in this Figure may be due to experimental error (the modulus values at the two temperatures differ by only 6%), or may be a genuine effect due to the dependence of modulus on temperature and pressure history[8].

At 33.9°C the material is in the midst of the dispersion region at atmospheric pressure (*Figure 3*). As pressure is applied it becomes glassy and less rate dependent. The curves of shear modulus, G, against pressure, P, at the different strain rates, $\dot{\gamma}$, have been cross-plotted as $\log_{10}G$ vs. $\log_{10}(\dot{\gamma})$ at constant P (*Figure 4*), and shifted horizontally to form a master curve (*Figure 5*) at 33.9°C and atmospheric pressure The shift factors ($\log_{10}a_p$) used are graphed against pressure in *Figure 6*. The mean slope is:

$$K = \frac{d(\log_{10}a_p)}{dP} = 5.7 \times 10^{-2}(MN/m^2)^{-1}$$

O'Reilly[4] derived an equation for K to describe dielectric

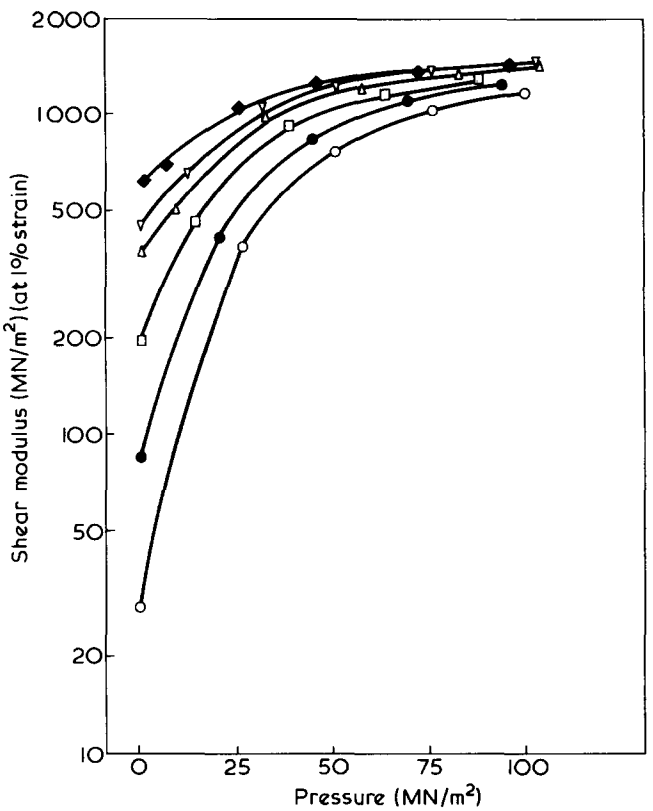

Figure 3 Shear modulus (1%) of PVAc at 33.9°C *versus* pressure. Strain rates X 10^4 (sec^{-1}): ○, 0.9; ●, 2.8; □, 8.0; △, 24; ▽, 76; ◆, 226

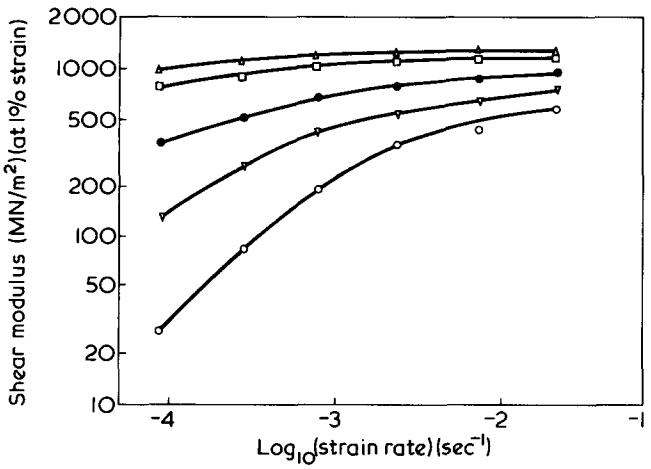

Figure 4 Shear modulus (1%) of PVAc vs. strain rate (double logarithmic plot). Pressures (MN/m^2): ○, 0.1, ▽, 12.5; ●, 25; □, 50; △, 75

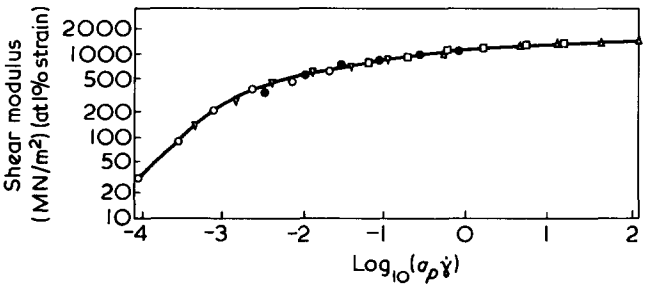

Figure 5 Master curve of shear modulus vs. $\log_{10}(a_p\dot{\gamma})$; symbols as for *Figure 4*. Data reduced to atmospheric pressure at 33.9°C using shift factors shown in *Figure 6*

data at various pressures and temperatures 60°–100°C on the basis of the WLF equation, with the non-linear compressibility of free volume necessary to fit his data:

$$K = \frac{b}{f_g + \alpha_f(T - T_g)}$$

where $b = 1.346 \times 10^{-3}$ $(MN/m^2)^{-1}$ = free volume pressure coefficient; $f_g = 0.023$ = fractional free volume at T_g; $\alpha_f = 5.3 \times 10^{-4}K^{-1}$ = coefficient of thermal expansion of free volume and $T_g = 301K$, the glass transition temperature.

This gives the value $K = 5.14 \times 10^{-2}$ $(MN/m^2)^{-1}$ at 34°C, in excellent agreement with the value found here. This is perhaps fortuitous in view of the assumptions and extrapolations involved.

We see in *Figure 6* that the rate of change of shift factor $\log_{10}a_p$ with pressure decreases at $P = 75$ MN/m^2. This may be because the material has not reached an equilibrium volume at the higher pressure; it is inevitable that measurements of shear modulus well into the glass region at times of the order of 10 sec, as used here, will be on material that is not in volume equilibrium, as is also true of the dielectric measurements[4]. Here, however, the use of the pressure-ramp gives a repeatable condition of the material[8], similar to a slow cooling.

Strength of the α relaxation. The nature of the α relaxation can be investigated through the strain rate dependence of the modulus as outlined in part 1. From the strain rate corresponding to the maximum value of $S = \partial G/\partial \ln\dot{\gamma}$, the dominant relaxation time at 33.9°C and atmospheric pressure can be seen in *Figure 5* to be $\theta_m = 4$ sec. The peak value of S in the transition, S_{max}, can also be used to esimate a peak value for the imaginary part of the complex modulus (see part 1), giving:

$$G''_{max} = 0.28\,G_m$$

at 34°C and 0.04 Hz where G_m is the glassy modulus.

The direct measurements of complex modulus[3] give:

$$G''_{max} = 0.23\,G_m$$

at 75°C and 2 MHz, indicating that this peak value changes little with temperature, as would be expected of a polymer obeying time–temperature superposition.

Stress–strain curves and yield

Figure 7 shows the highly rate-dependent stress–strain curves of the material in the transition region. A three de-

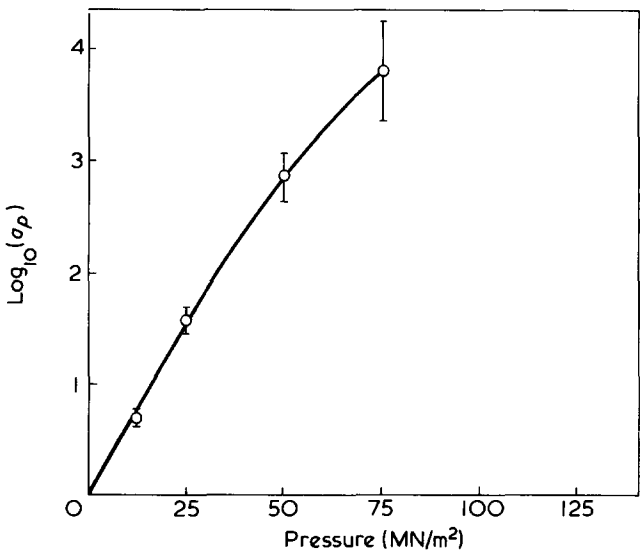

Figure 6 Pressure shift factors used for master curve in *Figure 5*

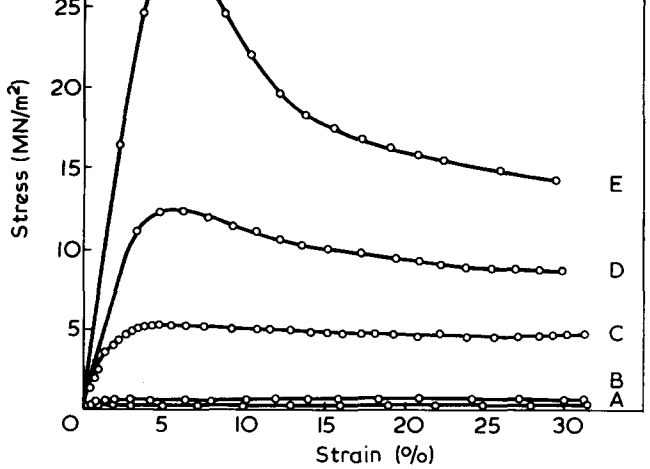

Figure 7 Constant strain rate stress–strain curves for PVAc at 33.9°C at atmospheric pressure. Strain rates (sec^{-1}): A, 4.54×10^{-5}; B, 3.04×10^{-4}; C, 3.03×10^{-3}; D, 1.36×10^{-2}; E, 7.43×10^{-2}

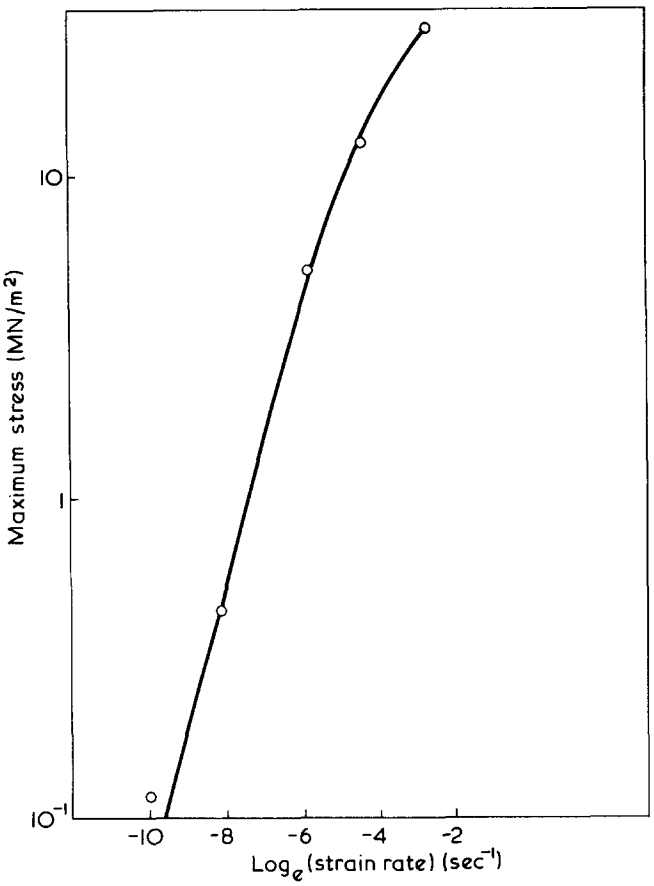

Figure 8 Maximum stress data from *Figure 7* vs. strain rate. Full curve deduced from Ree–Eyring equation: $\dot{\gamma}/\dot{\gamma}_0 = \sinh(\tau_y/\tau_0)$ with $\tau_0 = 8.7$ MN/m^2 and $\dot{\gamma}_0 = 6.1 \times 10^{-3}$ sec^{-1}

cade increase in strain rate produces an increase in secant modulus at 1% strain from 9 to 740 MN/m^2, and an increase in maximum stress from 0.28 to 27.7 MN/m^2. The characteristics are thus rubbery in the low strain rate region and glassy in the high. The curves at the two lowest strain rates show a rapid relaxation in the first 1 to 2% strain until a flow stress, τ_f, is reached, followed by a gradual linear increase in stress with strain. This linear increase has a slope of 0.4 MN/m^2, typical of the modulus of rubbers. Thus, after an initial viscoelastic relaxation of relaxation time about 10 sec, the stress is governed by a rubbery network, in which the junctions are produced by the chain entanglements which also produce the 'high molecular weight plateau' in the dependence of modulus on temperature[9]. This plateau modulus is found to be 0.3 MN/m^2, in reasonable agreement with the value found above.

The curves at the highest strain rates show a maximum stress, τ_m, followed by a yield drop. It can be seen from *Figure 7* that this yield process develops out of the small stress–small strain relaxation mentioned above. As previously[1], we test the applicability of the Ree–Eyring equation to this development. The yield stress, τ_y, given by τ_f or τ_m as appropriate, is plotted against ln(strain rate) in *Figure 8*. Also plotted is the Ree–Eyring equation for yield stress:

$$\dot{\gamma}/\dot{\gamma}_0 = \sinh(\tau_y/\tau_0)$$

where $\dot{\gamma}$ = strain rate. τ_0 and $\dot{\gamma}_0$ have been chosen to be 8.7 MN/m^2 and 6.1 x 10^{-3} sec^{-1}, respectively, to fit the measured variations of the yield stress over more than two orders of magnitude. Measurements of the glassy shear modulus of $G_u = 1300$ MN/m^2 can be used with these parameters to calculate an effective small strain relaxation time, θ_m:

$$\theta_m = \frac{\tau_0}{G_u \dot{\gamma}_0} \approx 1.1 \text{ sec}$$

This is quite comparable with the experimental value of θ_m derived from the modulus data in *Figure 5*, and so we can conclude, in contrast to the case of PP, that the yield process arises from a stress-dependent viscosity. This can be modelled, to a first approximation, over the whole of the experimental range of stresses by the Ree–Eyring equation. (This is in contrast to the data from PP where estimates of θ_m from small and large strain data using the Ree–Eyring equation differed by several orders of magnitude.)

Isochronal curves

The isochronal curves in *Figures 9, 10* and *11* show that the response is linearly viscoelastic up to high strains at low stresses and long times, but that as the stress τ_0 is reached so the material becomes non-linear, as would be expected from the Ree–Eyring equation. The basic form of the non-linear viscoelastic response is thus the simple one of a stress activated flow process.

A more detailed examination of the response, however, reveals various interesting phenomena. A plot of secant modulus, $G(\gamma)$ vs. strain (*Figure 11*) shows that there are extended regions of almost constant modulus at times longer than 100 sec, indicating an extended linear response at these times. At shorter times the non-linear stress-activated process causes the modulus to decrease as strain increases from its high initial value. This is in agreement with the basic response following the Ree–Eyring equation as described above. In addition to this response there appear to be two subsidiary phenomena, that of a rise in modulus at strains below about 4% and times less than 32 sec, and that of a sharp fall in modulus that occurs at strains less than 5% and times greater than 32 sec. Whilst these data appear anomalous, and the possibility of their being due to experimental error could not

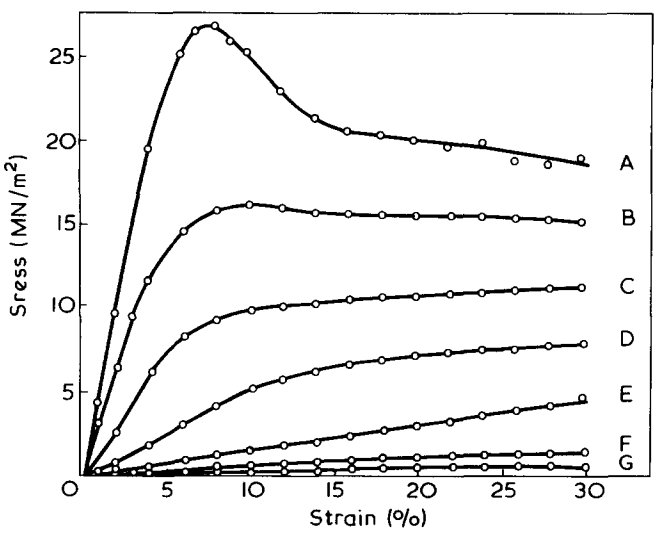

Figure 9 Isochronal stress–strain data. Temperature = 33.9°C. A, 1.0 sec; B, 3.2 sec; C, 10 sec; D, 32 sec; E, 100 sec; F, 320 sec; G, 1000 sec

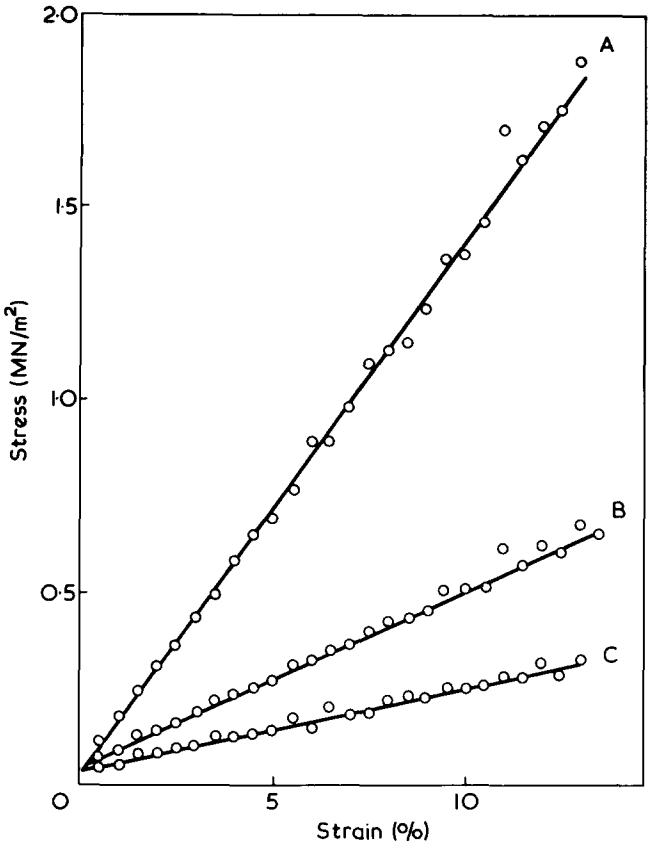

Figure 10 Detail of the isochronal stress–strain data at low stresses and long times. Temperature = 33.9°C. A, 100 sec; B, 320 sec; C, 1000 sec

be entirely excluded, we nonetheless propose to treat them as genuine phenomena and hope to show below that they can be thus explained in a manner more consistent with previous findings.

Strain hardening process at small strains. Let us examine the rise in modulus at strains below about 4% and times less than 32 sec (*Figure 11*). This strain hardening at relatively small strains has been already observed in data from the glass transition region in rubbers[11] and also in polypropylene[1], although in the latter at a level small enough to be due to experimental error. Strain hardening in rubbers is usually associated with fully extended chains and thus an exhaustion of available molecular configurations. To explain its occurrence at these low strains we might hypothesize the existence of temporary physical crosslinks in the glass transition region, giving a high effective crosslink density, and consequently a rapid strain hardening as chains become fully extended between these entanglements. However, as stress rises with strain this hardening process is swamped by the stress-activated flow associated with yield.

It can now be seen why this increase in isochronal modulus at small strains appears only in the region of rapid change of modulus with time. Suppose that there is a spread of energy barrier heights and hence relaxation times associated with the activated processes in the transition region, and let us crudely separate these into two classes, the 'fast' ones, with relaxation times shorter than the experimental time, and the 'slow' ones, with relaxation times longer than that of the experiment. As the transition is traversed by, for instance, reducing progressively the experimental time, as in *Figure 11*, the class of 'fast' relaxations shrinks, and that of 'slow' ones grows. In the glassy state all relaxations are 'slow', in the rubber state all are 'fast'. In between, there are some fast and some slow. It is exactly the 'slow' class that forms the entanglements cited above, and the 'fast' class that forms the short rubbery chains between. Thus the region of change over from mainly fast to mainly slow behaviour is the region in which both the rapid increase in modulus and the temporary, highly crosslinked networks occur.

This in turn shows that the build up of the yield process in the transition region (see *Figure 7*) is determined by the stress activated breakdown of the temporary entanglements. Thus the modulus at 1% strain and at 10 sec (see *Figure 11*) will be determined by low activation energy processes available at that strain, whereas the flow stress involves the higher energy processes as well. We see that, despite the broad description of the data at both low and high strains by the Ree–Eyring equation outlined above, the modulus and yield stress may not in detail be governed by a unique mechanism.

Strain softening at large strains. The second subsidiary phenomenon arising from the data of *Figure 11* is the sharp fall in modulus with increasing strain that occurs at strains less than 5% and at times greater than 32 sec. That this is not entirely due to error in the lowest strain rate test is demonstrated by the agreement between values of modulus at 1% strain as a function of time obtained here with the values of modulus as a function of frequency obtained in dynamic modulus measurements[3]. This sharp fall in modulus indicates a non-linear process operating at small strains which can also be seen in *Figure 10*. This Figure shows isochronal stress–strain curves at small strains for times of 100 sec and longer, which if extrapolated back to zero strain, intercept the stress axis at a stress of 0.05 MN/m^2. Examination of *Figure 8* also shows that the yield stress at the lowest strain

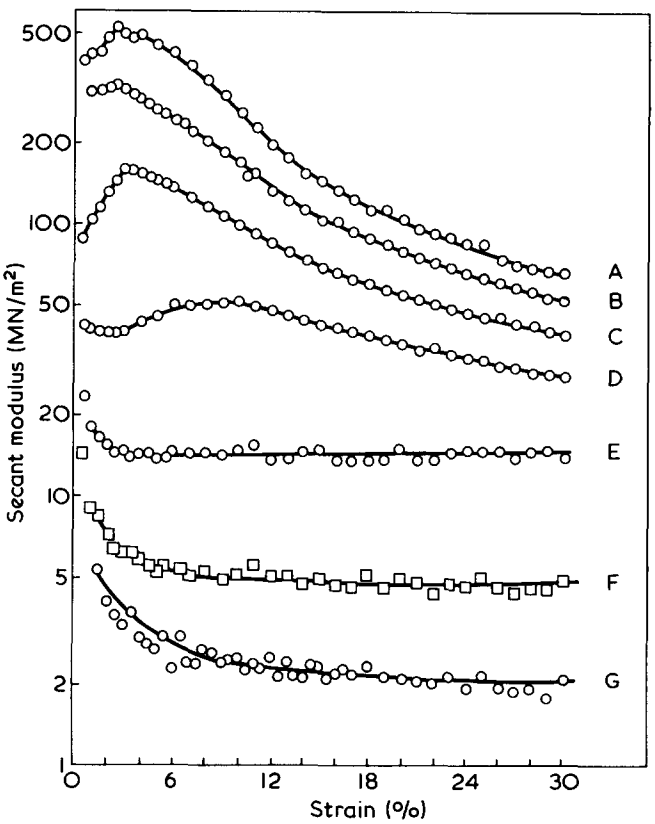

Figure 11 Secant modulus vs. strain at times indicated. Temperature = 33.9°C. A, 1.0 sec; B, 3.2 sec; C, 10 sec; D, 32 sec; E, 100 sec; F, 320 sec; G, 1000 sec

rate exceeds that predicted from the Ree–Eyring equation by 0.05 MN/m^2. We hypothesize a subsidiary activated process of flow stress 0.05 MN/m^2 acting in parallel with the main yield process in order to explain these findings. This process is not detectable at the higher strain rates and shorter times owing to its small magnitude. Thus as was found with polypropylene in part 1 the processes prevailing at high and at low strains may not be the same.

CONCLUSIONS

Measurements of time–pressure shift factors and of the peak value of the imaginary part of the complex modulus made in these experiments agree well with previous findings. These small strain measurements can be related approximately to the large strain (yield stress) data by means of the Ree–Eyring equation. However, the work in both parts of this study shows the difficulty, and perhaps also the inadvisability, of attempts to produce a global description of the non-linear viscoelastic properties of polymers. In place of more mathematically elaborate schemes proposed[12,13], which could in principle furnish a general theory of non-linear response, a description of particular processes has emerged. These processes are particular to the values of temperature, pressure, stress, strain and time under consideration, and to the relaxation transitions and morphology of the polymer.

In polypropylene the mechanical behaviour was seen (in Part 1, as elsewhere[7,1]) to be dominated by the β relaxation, but a simple quantitative modelling of this effect was apparently frustrated by the complexities of the response of a semicrystalline structure. The choice of PVAc, an amorphous material, in the α transition region was rewarded by a unified description of the modulus and yield stress data in the Ree–Eyring equation. Once again, however, examination of the finer details of the whole stress strain response seems to indicate that there may exist subsidiary processes that govern certain regions of the response.

We conclude that an understanding of both modulus and yield stress measurements can be had only by considering them in conjunction, as parts of the total non-linear response of the material, and that this response may be related to the structures and processes occurring in that material.

REFERENCES

1 Duckett, R. A. and Joseph, S. H. *Polymer* 1978, **19**, 837
2 McCrum, N. G., Read, B. E. and Williams, G. 'Anelastic and dielectric effects in polymeric solids', Wiley, New York, 1967
3 Williams, M. L. and Ferry, J. D. *J. Colloid Sci.* 1954, **9**, 479
4 O'Reilly, J. M. *J. Polym. Sci.* 1962, **57**, 429
5 McKinney, J. E. and Belcher, H. V. *J. Res. Nat. Bur. Stand. (A)* 1963, **67**, 43
6 Schmieder, K. and Wolf, K. *Kolloid Z.* 1953, **134**, 149
7 Duckett, R. A., Goswami, B. C., Smith, L. S. A., Ward, I. M. and Zihlif, A. M. *Br. Polym. J.* in press
8 Duckett, R. A. and Joseph, S. H. *Polymer* 1976, **17**, 329
9 Jones-Parry, E. and Tabor, D. *J. Mater. Sci.* 1973, **8**, 1510
10 Meares, P. 'Polymers: structure and bulk properties' Van Nostrand, New York, 1965
11 Schallamach, A., Sellen, D. B. and Greensmith, H. W. *Br. J. Appl. Phys.* 1965, **16**, 241
12 Lockett, F. J. 'Non-linear viscoelastic solids' Academic Press, London, 1972
13 Brereton, M. G., Croll, S. G., Duckett, R. A. and Ward, I. M. *J. Mech. Phys. Solids* 1974, **22**, 97
14 Yoon, H. M., Pae, K. D. and Sauer, J. A. *J. Polym. Sci.* 1976, **14**, 1611